Injection of protons and extraction of antiprotons at the Antiproton Decelerator

Ulrik Mikkelsen

Institute for Storage Ring Facilities, ISA, University of Aarhus,

DK–8000 Aarhus C, Denmark

and

PS-CA, CERN,

CH-1211 Geneva 23, Switzerland

E-mail: ulrik@dfi.aau.dk, ulrik.mikkelsen@cern.ch

March 26, 1998

Abstract

The optics and the basic parameters for extraction of 0.10 GeV/c $\overline{\mathrm{p}}$ and reverse injection of 3.57 GeV/c p in the Antiproton Decelerator (AD) are described.

1 Introduction

For the setting-up of the Antiproton Decelerator (AD), a relatively intense beam of protons of 3.57 GeV/c must be provided, $10^9 - 10^{10}$ particles per pulse. This can be done in two modes: reverse with respect to the direction of the antiprotons and clockwise by injection through the target zone. Only the former - which does not require change of polarity of the magnets in the machine - is considered in this study. It is done by a transport through the TTL2 loop, the 8000 line and the 7000 line followed by injection at the septum in section 53 of the AD and using the kickers in sections 50 and 35. For the extraction of antiprotons, only one kicker section is used since the magnetic rigidity of the 0.10 GeV/c $\overline{\mathrm{p}}$ is a factor 36 lower than for the protons - 0.33 Tm compared to 11.9 Tm.

In the following, numbers referring to distributions are based on $\pm 2\sigma$ values, ie. 95% of the beam.

2 Kickers and septum

Probably due to a large number of modifications and adjustments, several values can be found for the septum angle, ie. the difference between bearings of the QDC53 in the machine and the entry of DE.BHZ7010 in the 7000 line, see table 1. The value used for the present studies is that given by the Survey data [3].

	Angle [mrad]
Ref. [1]	130.68
Ref. [2]a	139.63
Ref. [2]b	113.43
Ref. [3]	129.62
Ref. [4]	129.6

Table 1: *Septum angles according to different sources.*

On the other hand, the 'septum jump' is 57.5 mm in [2] and found to be 58.2 mm from [3], a discrepancy which is hardly significant. The septum is not motorized.

	Angle, $\overline{\mathrm{p}}$ [mrad]	Angle, p [mrad]
Septum	117.06	116.57
Kicker, sect. 35	0	4.965
Kicker, sect. 50	9.67	4.965

Table 2: *'Magnetic' angles for kickers and septum*

The kicker angles are adjusted to give a good agreement of the new closed orbit with the values of $x = 58.2$ mm and $x' = 129.62$ mrad at the septum. The trajectory

of the beam between the first kicker and the septum is shown in figure 1. For proton injection the values are 4.965 mrad in each of the two kicker sections 35 and 50 and for antiproton extraction the kicker section 35 is kept at zero while section 50 gives a 9.67 mrad deflection. The recommended values are given in table 2 and conversion factors to obtain current can be found in appendix A.

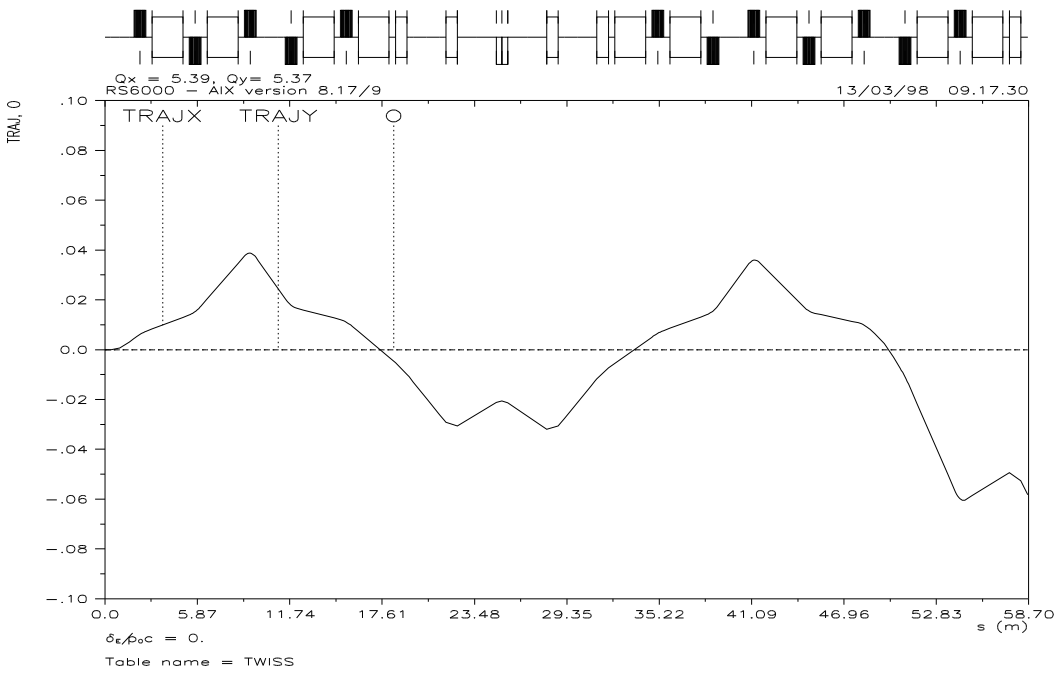

Figure 1: *Trajectory of the kicked beam from the 1st kicker to the septum. The excursion is given in m.*

The beamsize at the location of the septum is $\simeq 6 \times 6$ mm^2 for protons and antiprotons, assuming an emittance of $\varepsilon_h = \varepsilon_v = 5\ \pi$ mm·mrad in both cases. The momentum spread is taken as $\Delta p/p = 10^{-3}$ for antiprotons and $\Delta p/p = 10^{-4}$ for protons.

3 Optics

The matching in the case of $\overline{\mathrm{p}}$ was performed by use of MAD [5] including the part of the AD lattice from QFW50 to the septum [6] (values considered fixed in this study) and ending at the distribution magnet for the experiments, DE1.BHN 10. For the matching of the proton injection, the line was initiated at QFO105 in TT2 with continuation via the TTL2 loop, the transport lines 8000 and 7000 and the septum through the two kicker sections to QDW35.

The height difference of 3 mm of the beam exiting the 8000 line and the initial

direction of the 7000 line[1] was compensated by an adjustment of angles and tilts for the elements BTI8025 and BTI8002 along with a movement of the ATP.BHZ8000 along the 7000 line and thus a slight modification of its deflection angle, see table 3. The geometry of the line was checked by use of BEATCH [7] which leads to results slightly different from those obtained by a MAD survey when tilted dipoles are used.

x	y	z	α
1732.226562	2145.594619	2436.13312	274.98

Table 3: *Intersection point (x, y, z) in the 2000 coordinates and angle in mrad between the 7000 and 8000 lines.*

3.1 Protons

In some cases it is not possible to obtain a perfect match at both ends of the line in question, while maintaining an acceptable beam-size throughout the beam transport line. The emittance increase arising from such a mismatch and the following filamentation in the ring (thus, only relevant here for proton injection) is found from [8]

$$\varepsilon_2 = \frac{1}{2}(\frac{\beta_1}{\beta_2} + (\alpha_1 - \alpha_2\frac{\beta_1}{\beta_2})^2\frac{\beta_2}{\beta_1} + \frac{\beta_2}{\beta_1})\varepsilon_1 \tag{1}$$

where the subscripts denote expected (1) and mismatched (2) values. However, due to the large number of elements available for the match, a perfect solution could be obtained.

In figure 2 is shown the beamsize as a result of the optics calculated for the proton injection, beginning at the 8000 line (QFO8090), traversing the large deflection magnet which connects the 8000 and 7000 line and ending at the septum. The maximum value of the β-function is 40 m in both planes, corresponding to a beamsize of 14 mm. The vertical dispersion, D_y, and its derivative, D'_y, at exit of the last tilted bend, BTI8002, are matched to zero such that the effect of the residual dispersion is negligible as shown below.

In figure 2 is shown the total size of the beam

$$x = \sqrt{\varepsilon\beta + D^2(\frac{\Delta p}{p})^2} \tag{2}$$

and the contribution from the dispersion, $x_D = D \cdot \Delta p/p$, as a function of position along the lines. Note that MAD assumes a positively charged particle when displaying the quadrupole sequence.

The expected and matched values at the input of the AD were in perfect agreement. A horizontal acceptance, defined as $A = \pi r^2_{\rm min}/\beta_{\rm max}$, of 16 π mm·mrad was obtained

[1]This difference seems to have arised due to different periods of construction for the two lines.

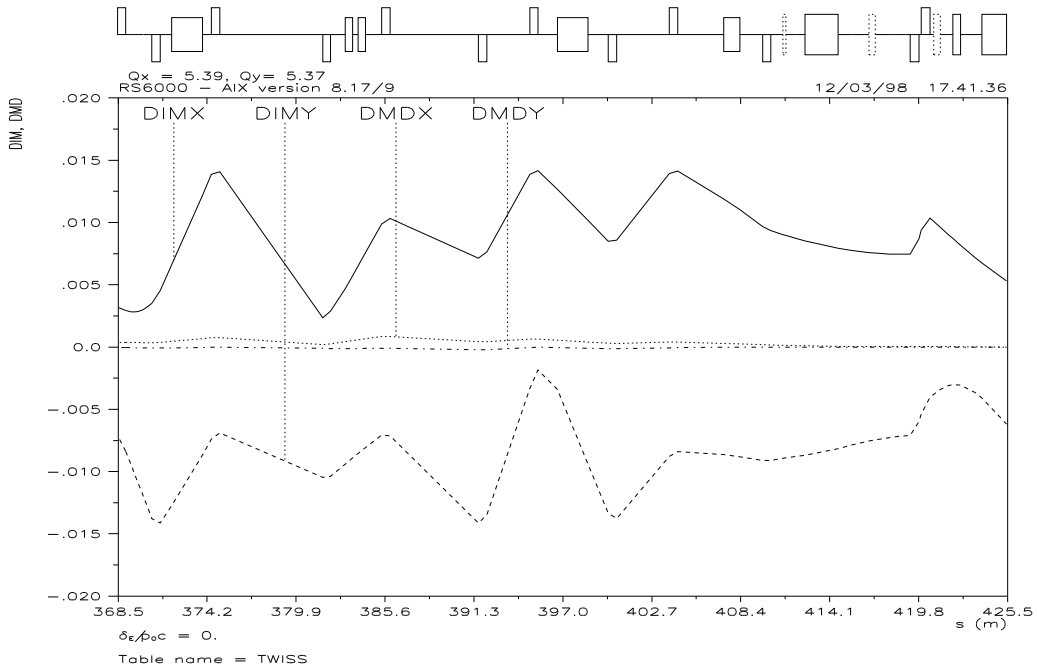

Figure 2: *Total beamsize in m and the contribution from dispersion for proton injection through the 8000 and 7000 lines.*

with the limitation being at the $\simeq 40\times110$ mm^2 (h×v) aperture of the BTI8002 magnet. In vertical the acceptance has a minimum of 24 π mm·mrad at the quadrupole 8020. The gradients and currents for the elements used are given in table 12 in appendix A.

In order to reduce the contribution from the vertical dispersion, the 'dispersion invariant'[2] (which is only invariant in the absence of dipole components in the particular direction), ε_D, must be small at the exit of the last tilted dipole, BTI8002

$$\gamma D^2 + 2\alpha DD' + \beta D'^2 = \varepsilon_D \tag{3}$$

where α, β, γ are the usual Twiss parameters. For the present case, $\varepsilon_D = 3 \cdot 10^{-17}$ π mm·mrad, and using $\Delta p/p \simeq 10^{-4}$ and $D = \sqrt{\beta\varepsilon_D}$ in eq. (2) which leads to

$$y \simeq \sqrt{\varepsilon\beta}(1 + \frac{\varepsilon_D}{2\varepsilon}(\frac{\Delta p}{p})^2) \tag{4}$$

one obtains a contribution to the vertical beam size in the AD originating from the vertical dispersion which is clearly by far negligible. The contribution to y' is equivalent and thus the expected transverse emittance increase is

$$\Delta\varepsilon = \varepsilon_D(\frac{\Delta p}{p})^2 \tag{5}$$

[2]I thank Jean-Yves Hemery for drawing my attention to this parameter.

which is completely negligible even if $\Delta p/p = 10^{-2}$. This, of course, is only true in the absence of coupling between the vertical and horizontal planes.

All the quadrupoles in the 8000 line have equivalent magnetic length 0.537 m and a current limit of 150 A. In the 7000 line the 7030 and 7020 have an equivalent magnetic length of 0.559 m (at 750 A) with a limit of 4000 A and 3000 A, respectively, in the pulsed mode for protons, while the limit is 100 A each in the DC mode for antiprotons. The conversions from integrated gradient to current and vice-versa are given by fifth-order polynomials found by a fit to measured values [10].

3.2 Antiprotons

Matching of the experimental lines, starting at the intersection point of the 7000 and 8000 lines in ATP.BHZ8000, was performed by M. Giovannozzi [11] before the Twiss parameters of the AD were known to better than 20%. Therefore the transfer line 7000 and the common part of the lines for the experiments (from ATP.BHZ8000 to DE1.BHN10) had to be matched once the final AD lattice was known [12].

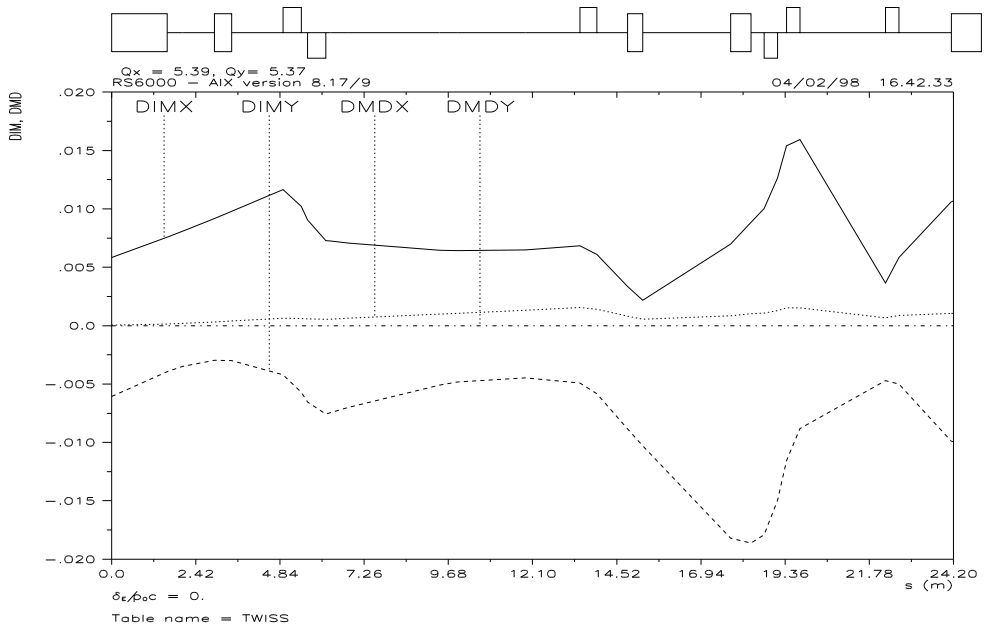

Figure 3: *Total beamsize in m and the contribution from dispersion for antiproton extraction from the septum through the 7000 line to the distribution magnet, DE1.BHN10.*

The beam size as a result of the matching, from the septum to the distribution magnet, DE1.BHN10, is shown in figure 3. A conservative value of 5 π mm·mrad has been chosen for the emittance in both planes, since at the present stage the influence of residual gas and intrabeam-scattering in the ring at 0.1 GeV/c is not known to

better than a factor $\simeq$ 2 with the current minimum emittance value being $\simeq$1.5 π mm·mrad [13].

	Int. gradient [T]	Current [A]
QF7030	0.2574	26.72
QD7020	-0.2310	-23.92

Table 4: *Gradients for the antiproton extraction to ATHENA, ATRAP and ASACUSA through the 7000 line.*

The optics is based on reversed polarity of the quadrupoles with respect to the proton injection and the optics to be used for the RFQ (see below). This is done to be able to decrease the beam size in the transport through the 7000 line while matching to the pre-defined parameters for the experimental lines. Thus the 7020 and 7030 become defocusing and focusing, respectively.

The acceptance is 45 π mm·mrad horizontally and 44 π mm·mrad vertically for the septum-to-DE1.BHN10 line. The limit is at the 70 $\times$ 45 mm^2 (h$\times$v) aperture of the 7020 and 7030 quadrupoles. The horizontal dispersion is nowhere larger than 1 m.

3.3 Antiprotons - RFQ

For the optimal deceleration in an RFQ, a buncher is necessary to accomodate the beam in a time-varying structure. This introduces a large momentum spread such that the dispersion and its derivative must be zero in both planes at exit of the distribution magnet, DE1.BHN10, to avoid excessive blow-up of the beam. The horizontal dispersion invariant, eq. (3), was matched to become $\varepsilon_D = 3 \cdot 10^{-12}$ m, which leads to a horizontal dispersion and derivative being both of the order $\simeq 10^{-6}$ [m] at the input of the buncher.

The acceptance is 20 π mm·mrad in both planes.

	Int. gradient [T]	Current [A]
QD7030	-0.1375	-13.99
QF7020	0.1299	13.19

Table 5: *Gradients for the antiproton extraction to the RFQ of ASACUSA through the 7000 line.*

3.4 Alternative lattices for antiprotons

In order to compensate the blow-up of the beam in the machine arising at low energy, the beam is subjected to electron cooling. The effect of electron cooling may be enhanced by having a large dispersion and therefore two different lattices were tried, one

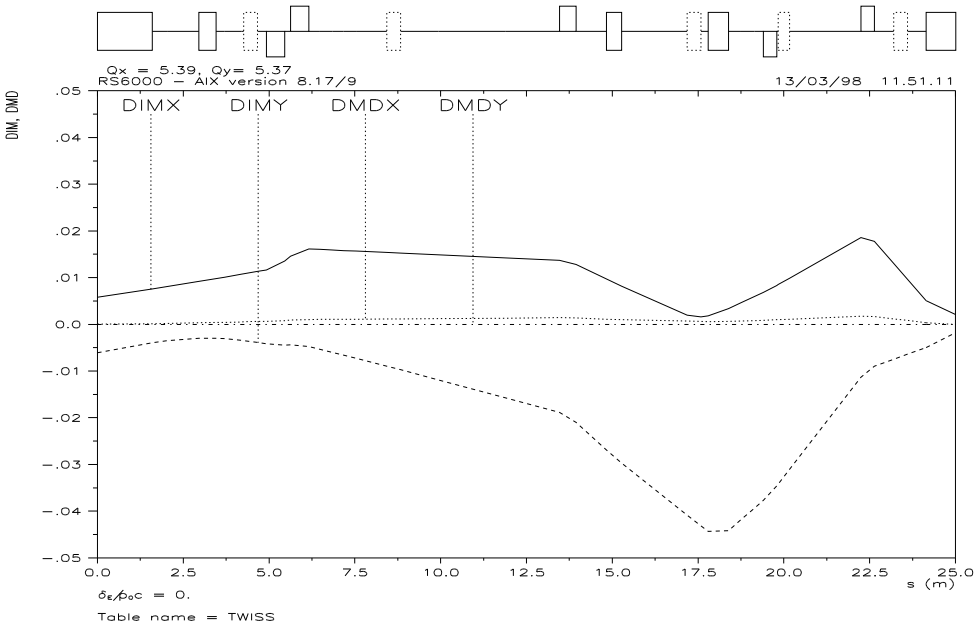

Figure 4: *Total beamsize in m and the contribution from dispersion for antiproton extraction from the septum through the 7000 line to the distribution magnet, DE1.BHN10, for the optics to be used with an RFQ in the ASACUSA experiment.*

with a dispersion of $D_x^{\rm EC} = -4$ m at the site of the electron cooler and one with a dispersion of 2 m [6], which can be compared with 0.17 m for the 'standard' solution. At the entrance of the septum, the dispersion changes from 0.044 m ('standard' solution) to 2.7 m ($D_x^{\rm EC} = -4$ m) and 0.73 m ($D_x^{\rm EC} = 2$ m). The Twiss parameters change by up to 50 %.

In table 6 are shown the focal sizes obtained by matching *only* the common part between the septum and the distribution magnet, DE1.BHN10. In other words, the quadrupole strengths in the lines have not been changed with respect to the 'standard' setting, such that the quoted focal values are not perfectly optimized and therefore represent a slightly pessimistic view. This bears out eg. in the case of $D_x^{\rm EC} = -4$ m for the DE3 line where the horizontal focal size is dominated by a residual dispersion of 1.6 m ('standard': 0.7 m).

The possibility of using these lattices in the context of the RFQ was not studied in detail with respect to stability due to eg. dipole errors. However, the requirement of zero dispersion and matching to the correct input Twiss parameters was in both cases manageable without compromising the maximum value of the β-functions.

As a conclusion, both of the mentioned AD lattices seem feasible from the point of view of the preliminary study of the extraction and experimental lines. However, adjustments for the $D_x^{\rm EC} = -4$ m solution must be applied to reduce the residual

	x_{-4}	y_{-4}	x_2	y_2	x_0	y_0
DE1	0.14	0.47	0.17	0.47	0.18	0.47
DE2	0.26	0.38	0.24	0.38	0.24	0.38
DE3	2.27	1.61	1.85	1.62	1.77	1.62
DE4	0.77	1.40	0.64	1.41	0.61	1.41

Table 6: *Horizontal and vertical focal sizes in mm for the alternative optics with* $D_x^{\rm EC} = -4$ *m,* $D_x^{\rm EC} = 2$ *m and the 'standard' solution with* $D_x^{\rm EC} \simeq 0$ *m, see text for details.*

dispersion at the focus of DE3.

4 Closed orbit distortion and instability

The normalized closed orbit distortion has been found to be ± 15 mm in the horizontal plane and ± 5 mm in the vertical plane [14]. This value, measured at a β of 12 m, corresponds to a surface in phase-space[3] of 19 π mm·mrad horizontally and 2 π mm·mrad vertically. Most likely, the beam will appear in approximately the same spot within this surface over a few hours, but it may change position eg. following a restart of the AD.

As a consequence of the variation of the kick-strength from one shot of antiprotons to the next about 1 minute later, the effective overall emittance will consist of a part from this variation which can not be compensated, $\Delta\varepsilon$, and the physical emittance. This extra contribution was simulated and found to be in agreement with the expected behaviour according to

$$\Delta\varepsilon = \frac{\pi}{2}\beta\theta^2(\frac{\Delta B}{B})^2 \tag{6}$$

where $\beta \simeq 7$ m is the value of the beta-function at the kicker, θ the kick-angle and $\Delta B/B$ the variation of the kick strengths. The values of the β-functions at the kicker section 50 are (β_x, β_y)=(7.2 m, 6.4 m) and at the septum: (6.8 m, 7.4 m) for $\overline{\rm p}$ and (5.6 m, 7.6 m) for p. Even with $\Delta B/B = 10^{-2}$ and additional, uncorrelated, relative errors of $5 \cdot 10^{-4}$ on the quadrupoles and dipoles downstream of the kicker, the contribution is small ($\simeq 0.8$ π mm·mrad) compared to the physical emittance of $\simeq 5$ π mm·mrad. Relative errors of $1.1 \cdot 10^{-3}$ on the dipoles and quadrupoles downstream the kicker leads to an additional emittance of $\simeq 5$ π mm·mrad.

The influence from the quadrupoles can be found from [15] $\varepsilon' = \varepsilon(\chi + \sqrt{\chi^2 - 1})^{1/2}$ where $\chi = \frac{1}{2}(\beta_2\gamma_1 + \beta_1\gamma_2 - 2\alpha_1\alpha_2)$ which in the thin-lens approach can be approximated as

$$\chi \simeq 1 + \delta = 1 + \frac{1}{2}(\frac{\beta_0}{f} \cdot \frac{\Delta f}{f})^2 \tag{7}$$

[3]The so-called effective overall emittance.

Here, subscripts 1 and 2 denote two different transformations of the $\beta_0, \alpha_0, \gamma_0$ through quadrupoles of focal lengths f and $f + \Delta f$, respectively and ε' is the phase-space circumscribing the emittance of both. For δ small, the emittance increase is $\varepsilon' - \varepsilon = \Delta\varepsilon \simeq \sqrt{\delta/2}$, ie.

$$\Delta\varepsilon \simeq \frac{1}{2}\frac{\beta_0}{f} \cdot \frac{\Delta f}{f} \tag{8}$$

which bears some resemblance to eq. (6). By use of typical values, β_0=7 m, f=0.8 m and $\Delta f/f = 10^{-3}$, this leads to $\varepsilon'/\varepsilon \simeq 1.0044$ for one quadrupole.

5 Monitoring and control in the transfer lines

The acceptance of the 7000 line and the position of the MWPCs should enable the steering of the beam to achieve complete transmission. At both the MWPCs, the acceptances are significantly larger than the expected (pessimistic) phase-space surface arising from the closed orbit distortions. The horizontal steering is performed by use of a combination of the septum, the DE.BHZ7010 and the DE.DHZ7041. Vertical steering is enabled by DE.DVT7013 and DE.DVT7042.

For the 8000 line, the steering magnets are the DHZ8052 and DHZ8009 (horizontal) and the DVT8048 and DVT8022 (vertical). A scintillation screen to monitor the steering before the 275 mrad deflection in ATP.BHZ8000 is inserted between the BTI8002 and the ATP.BHZ8000.

The phase advances are given in table 7.

	DE.MWPC7015	DE.DHZ7042	DE.DVT7042	DE.MWPC7046
horizontal	0.012	0.108	0.152	0.248
vertical	0.112	0.328	0.376	0.496

Table 7: *Phase advances (in units of $\pi/2$) between DE.DVT7013 and other steering and monitoring elements in the transport line 7000 for antiprotons to the 4 experimental lines.*

The Multi-Wire Proportional Chambers are monitors with 100 wires in both planes separated by 1 mm. These can be connected in such a way as to give resolutions of 2, 4 or 6 mm in 16 channels. Reconnection is fairly easy and cheap [16].

The distance between the two MWPCs in the 7000 line is 4.16 m. The angular resolution can be found from the angle, x_1', which at DE.MWPC7015 separates two beams incident a distance x_0 apart at both chambers

$$x_1' = x_0 \frac{1 - \sqrt{\beta_2/\beta_1}(\cos\Delta\mu + \alpha_1 \sin\Delta\mu)}{\sqrt{\beta_1\beta_2}\sin\Delta\mu} \tag{9}$$

	A_h	A_v
DE.MWPC7015	10	84
DE.MWPC7046	30	43

Table 8: *Acceptances [π mm·mrad] for the two MWPCs in the 7000 line by use of 2 mm resolution.*

where $\Delta\mu$ is the phase advance between the detectors and β_i and α_i the Twiss parameters at the i'th chamber. For $x_0 = 2$ mm this leads to the values 1.2 mrad and 1.3 mrad at DE.MWPC7015 where the divergence is 1.3 mrad and 1.7 mrad for the horizontal and vertical planes, respectively. The acceptances of the chambers are given in table 8 at the first and second MWPC for the case of antiprotons.

Turning off the quadrupoles in the 7000 line leads to tolerable beam sizes at the ATP.BHZ8000 magnet: $\beta_x = 85$ m and $\beta_y = 46$ m, corresponding to 21 mm and 15 mm, respectively.

A fast beam transformer, DE.TFA7044, is kept in the 7000 line and a newly designed, extra-sensitive beam transformer [17], DE.TFA7049, is intended to be inserted just upstream of the ATP.BHZ8000 magnet to cope with very low intensities as anticipated for commissioning with $\overline{\mathrm{p}}$.

6 Vacuum issues

To separate the vacuum of the TTL2 parts of the proton transport from the vacuum of the AD, two thin windows of each 100 μm Al are to be inserted. The emittance increase following this is found from eq. (6) with $\theta^2 = \theta^2_{\mathrm{RMS}}$ and $\Delta B/B = 1$ [8][4], where θ^2_{RMS} is the mean square angle arising from the multiple Coulomb scattering . The increase in emittance is relatively small, of the order $\Delta\varepsilon \simeq 0.5\ \pi$ mm·mrad, with the separation situated immediately upstream of the ATP.BHZ8000 where the β-functions in both planes are 15 m.

Finally, to separate the vacuum of the experiments from the vacuum of the machine, a valve of 63 mm inner diameter is to be introduced downstream DE.MWPC7046. This valve has a short closing-time (13 ms $\simeq$ 4.3 m of propagating air) allowing it to be used as a safety-valve in the event of rupture in one of the experiments [19]. It does not present a limitation to the acceptance of the lines with the optics foreseen.

[4]This is what one would expect, since for a magnet $\theta\Delta B/B$ is a measure of the uncertainty in deflection and in the case of multiple Coulomb scattering, this uncertainty is measured by θ_{RMS}. The same result is obtained by addition of the divergence and scattering in quadrature.

7 Conclusion

The beam transports through the 7000 and 8000 lines have been studied and suitable solutions have been found for the optics in both lines. The main objectives were to obtain a good match to the constraints given while preserving a small beam size throughout the lines in order to increase the acceptance and to keep the influence of errors at a minimum.

Furthermore, the sensitivity of the extraction of antiprotons on the reproducibility of the strength of the kick was studied and found to be relatively small.

Finally, two alternative lattices with non-zero horizontal dispersion at the site of the electron cooler were studied and found to be feasible.

8 Acknowledgment

The definition of the beam lines and the first attempts on the optics was performed by Claude Metzger [9] whom I thank for assisting in the definition of the constraints and for his help to overcome the obstacles encountered. I thank also Massimo Giovannozzi and Jean-Yves Hemery for providing efficient MAD tools and for valuable comments in the process. Furthermore, as evidenced by the References below, private communication with a number of people from the PS (and EST) Division has been very useful and appreciated.

Part I
Appendix A

	Antiprotons	Antiprotons - RFQ	Protons
Hor. acceptance [π mm·mrad]	45	20	16
Ver. acceptance [π mm·mrad]	44	20	24
Hor. maximum $\beta_{\max,x}$ [m]	50	68	40
Ver. maximum $\beta_{\max,y}$ [m]	69	393	40
Hor. dispersion, $D_{\max,x}$ [m]	1.5	1.8	8.6
Ver. dispersion, $D_{\max,y}$ [m]	0	0	2.3
Emittance [π mm·mrad]	5	5	5
Momentum spread $\Delta p/p$	10^{-3}	10^{-3}	10^{-4}

Table 9: *Main parameters for the optics discussed in this note.*

	0.100 GeV/c	3.575 GeV/c
Ejection septum [2]	205.7 mrad/kA	5.753 mrad/kA
Correction dipoles [4]	15.87 mrad/A	0.444 mrad/A
Ejection kickers 35-1,50-2 [20]	22.60 mrad/kA	0.632 mrad/kA
Ejection kickers 35-2,50-1 [20]	24.91 mrad/kA	0.697 mrad/kA
BHZ7010 [10]	0.869 mrad/A	22.74 mrad/kA
Q7020 [10]	35.42 m·A	1259.3 m·A
Q7030 [10]	35.49 m·A	1261.8 m·A

Table 10: *Conversion factors (assuming linearity around expected values) for some elements relevant for operation with antiprotons and protons. Values, α, for the quadrupoles are variation of focal length, $f = 1/kl = \alpha/I$.*

	Horizontal	Vertical
BHZ8000	0.2603 mrad/A	-
BTI8002	0.03633 mrad/A	0.2620 mrad/A
BTI8025	0.3638 mrad/A	0.2590 mrad/A
BTI8055	0.02675 mrad/A	0.15617 mrad/A
BTI8056	0.02668 mrad/A	0.15618 mrad/A
BTI8075	0.5058 mrad/A	0.1439 mrad/A
Q8***	215.73 m·A	215.73 m·A

Table 11: *Conversion factors (assuming linearity around expected values) for some elements relevant for operation with protons. Values, α, for the quadrupoles are variation of focal length, $f = 1/kl = \alpha/I$.*

	Gradient [T/m]	Current [A]
QF2615	3.3161	35.319
QD2610	-3.6859	-39.261
QF2605	6.3140	67.430
QF8090	4.3412	46.258
QD8080	-8.0361	- 86.027
QF8070	7.9079	84.639
QD8060	-3.9088	-41.639
QF8050	6.3794	68.134
QD8040	-7.9662	-85.271
QF8030	5.4808	58.469
QD8020	-7.3832	-79.964
QF8010	3.7642	40.097
QD8001	-1.1324	-12.026
QD7030	-12.212	-740.05
QF7020	12.063	730.35
	Angle [mrad]	Current [A]
BHZ8000	274.98	608.73
BTI8002	140.42	419.55
BTI8025	276.23	384.1
BTI8055	46.62	210.99
BTI8056	46.62	210.99
BTI8075	264.52	360.1

Table 12: *Gradients, angles and currents for the reverse proton injection through the 8000 and 7000 lines.*

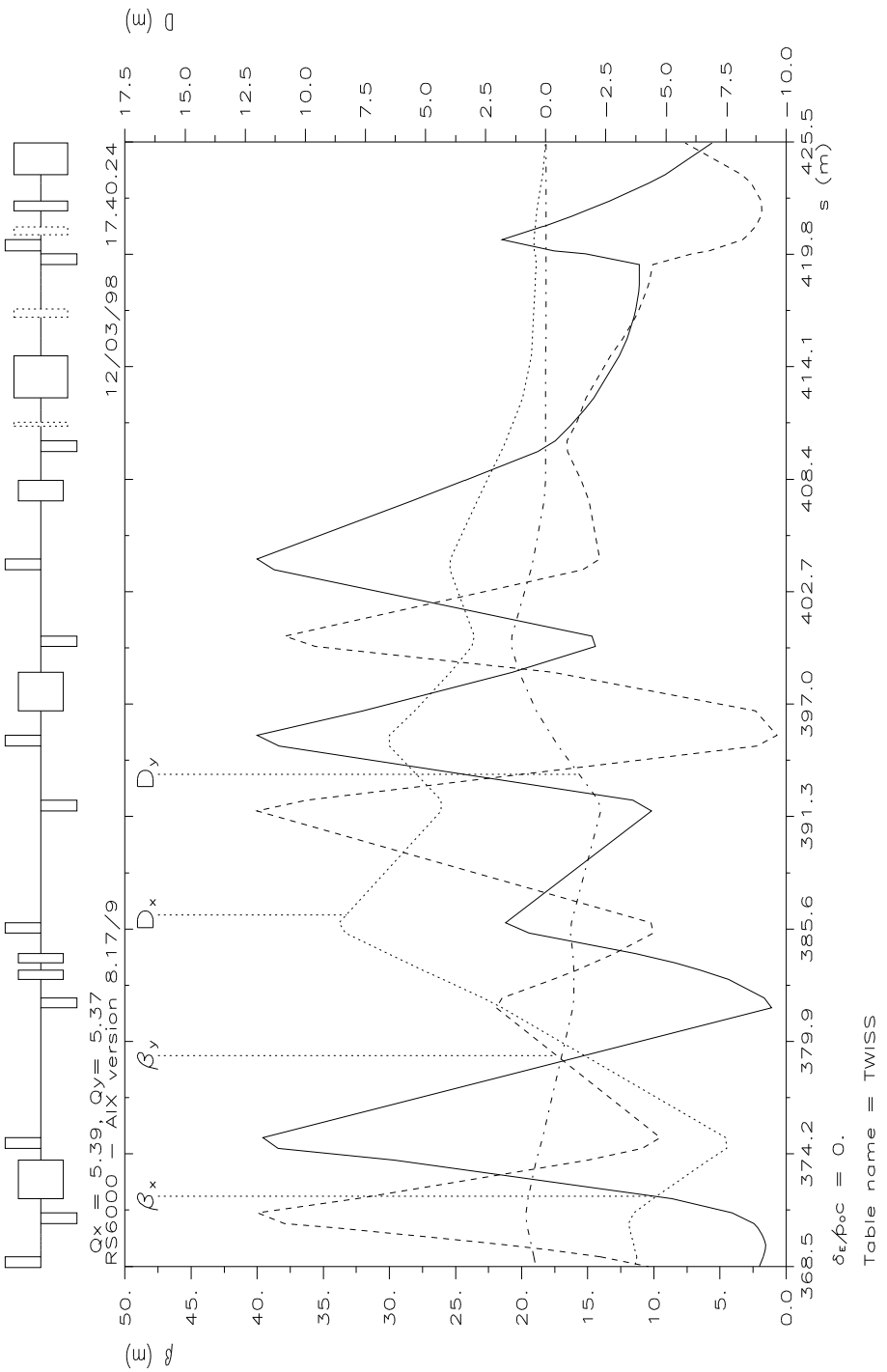

Figure 5: *Optical functions for proton injection through the 8000 and 7000 lines.*

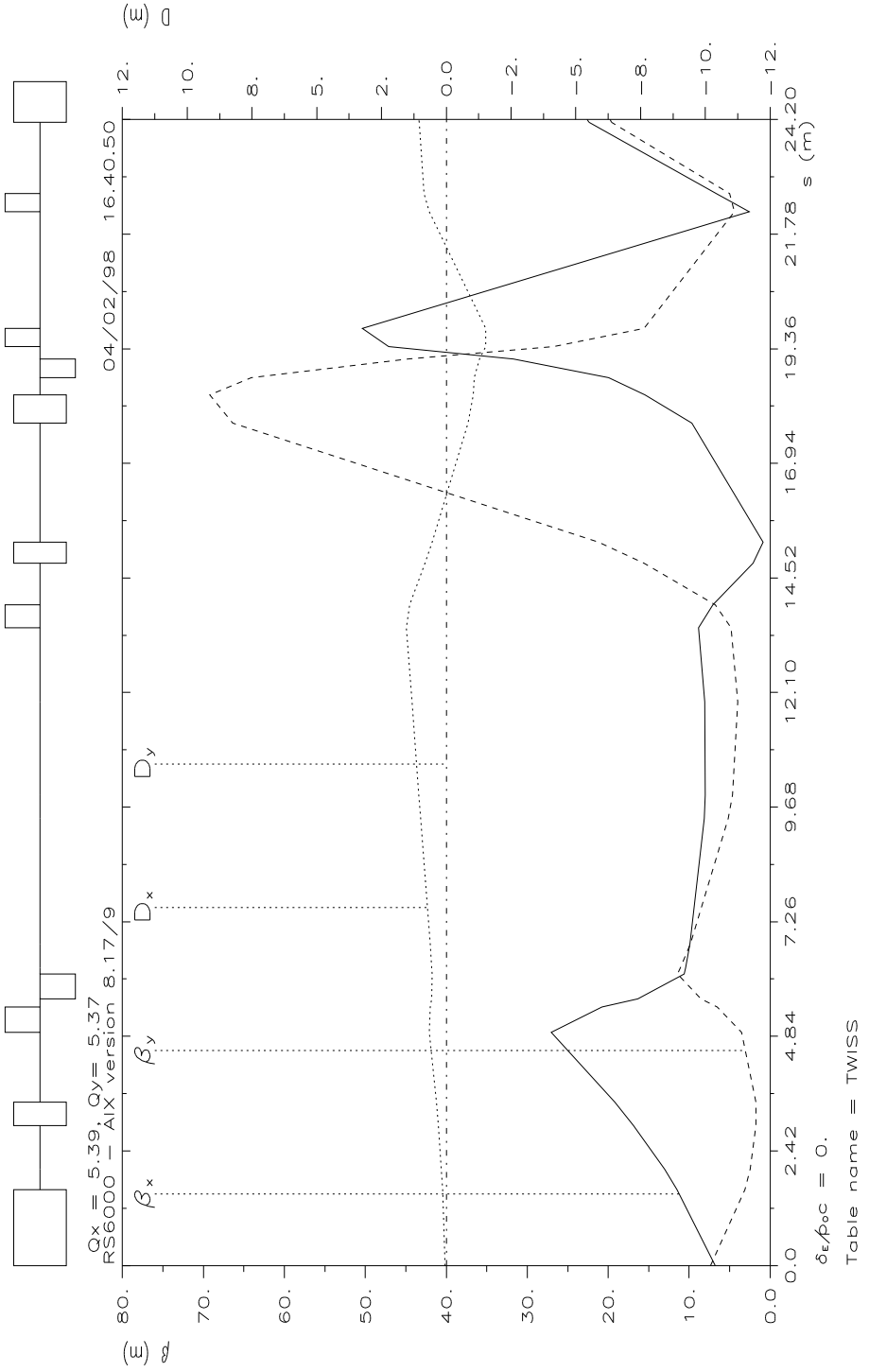

Figure 6: *Optical functions for antiproton extraction from the septum through the 7000 line to the distribution magnet, DE1.BHN10.*

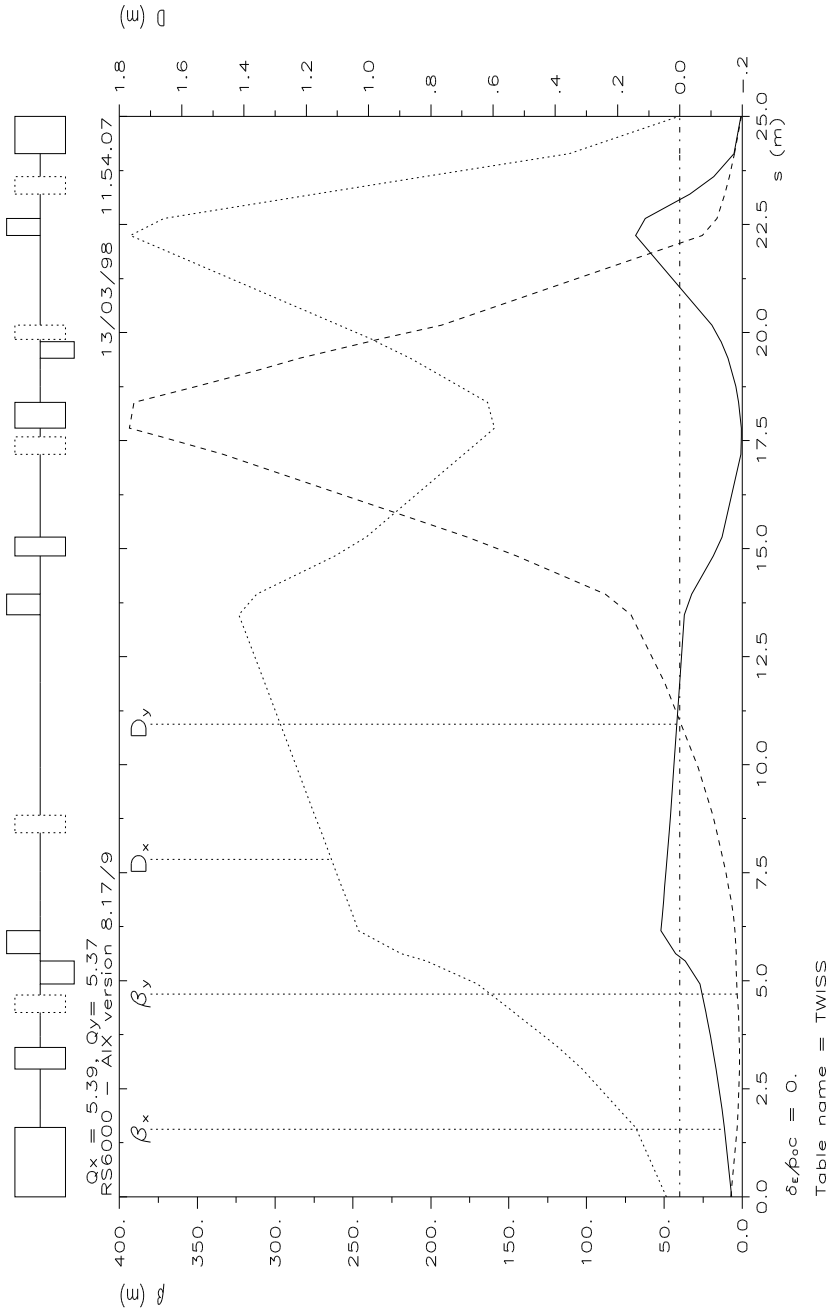

Figure 7: *Optical functions for antiproton extraction from the septum through the 7000 line to the distribution magnet, DE1.BHN10, for the optics to be used with an RFQ in the ASACUSA experiment.*

Figure 8: *Survey file for the 7000 and 8000 lines, generated such as to obtain agreement with coordinates given in [3].*

References

[1] H. Koziol and S. Maury, CERN/PS 95-15 (AR/BD)

[2] R. Valbuena, PS/PA Note 89-2, a) p. 10, b) p. 14

[3] Survey data as of 15.06.89

[4] S. Maury, private communication, 1997, value used in TRANSPORT

[5] H. Grote and F.C. Iselin, Methodological Accelerator Design (MAD), version 8.17, CERN/SL/90-13 (AP)

[6] P. Belochitskii and R. Giannini, private communication, 1998

[7] T. Dobers, private communication, 1998

[8] P.J. Bryant, CERN/PS 94-01, CAS General, Vol. I, p. 219-238

[9] C. Metzger, PS/CA/Note 97-17

[10] Ph. Cartier, E. Chinchio, G. Suberlucq, CERN Internal note, 25.08.87
E. Chinchio, G. Suberlucq, PS/PA/MA/Note 88-9
N. Siegel, CERN Memo SPS/ABT/TR/NS/80-199

[11] M. Giovannozzi, private communication, 1997

[12] R. Giannini, private communication, 1997

[13] N. Madsen, private communication, 1998

[14] C. Carli, private communication, 1998 and CERN/PS 97-35 (HP)

[15] C. Bovet, R. Gouiran, I. Gumowski, K.H. Reich, CERN/MPS-SI/Int. DL/70/4

[16] G. Molinari, private communication, 1998

[17] F. Pedersen, private communication, 1998

[18] S. Baird *et al.*, CERN/PS 96-43 (AR)

[19] M. Brouet, private communication, 1998

[20] K.D. Metzmacher and L. Sermeus, PS/BT/Note 87-11